AE-252
UDC 531.717.1:
539.122 (083.57)

AE-252

Nomogram for Determining Shield Thickness for Point and Line Sources of Gamma Rays

C. Jönemalm and K. Malén

AKTIEBOLAGET ATOMENERGI
STOCKHOLM, SWEDEN 1966

NOMOGRAM FOR DETERMINING SHIELD THICKNESS FOR POINT AND LINE SOURCES OF GAMMA RAYS

C. Jönemalm and K. Malén

Abstract

A set of nomograms is given for the determination of the required shield thickness against gamma radiation. The sources handled are point and infinite line sources with shields of Pb, Fe, magnetite concrete ($\rho = 3.6$), ordinary concrete ($\rho = 2.3$) or water. The gamma energy range covered is 0.5 - 10 MeV. The nomograms are directly applicable for source and dose points on the surfaces of the shield. They can easily be extended to source and dose points in other positions by applying a geometrical correction. Also included are data for calculation of the source strength for the most common materials and for fission product sources.

Printed and distributed in October 1966.

LIST OF CONTENTS

1. Introduction

The most common problem in shielding calculations is the estimation of the shield thickness when activating flux, activated material, shield material and allowed dose rate are known. There exist nomograms for estimation of dose rate when source strength, shield thickness and material are known (e.g. [1]). However, nomograms of this type are not easily applied in the reverse case when the shield thickness is wanted. In order to facilitate the determination of shield thicknesses for point and line sources a new type of nomogram has been prepared in which the previously mentioned drawbacks have been avoided. This set covers gamma energies between 0.5 and 10 MeV and the following materials: Pb, Fe, magnetic concrete (ρ = 3.6 g/cm^3), ordinary concrete (ρ = 2.3 g/cm^3) and water.

The use of the nomograms can be extended even to volume sources, as these in most cases can be approximated by one or more point or line sources. In the nomograms the escape probability is unity, which may be considered true in many practical problems. If it is less than unity the source should of course be reduced by this factor. It would have been desirable to make the nomograms valid for an arbitrary distance between source and dose point. To avoid making the nomograms too complicated this distance is taken equal to the thickness of the shield (R = x. Fig. 2). However, the nomograms can also be used when R>x by applying a geometrical correction described later.

2. Determination of the dose rate outside a shield

For preparing the nomograms the usual methods for calculating dose rate from point and line sources have been used [2]. Thus for a point source we have used

$$D = \frac{S_o \cdot B(\mu x) \cdot e^{-\mu x} \cdot k}{4\pi R^2} \qquad (1)$$

and for a line source

$$D = S_L \cdot k \, \frac{A_1 F[\frac{\pi}{2};\ \mu x(1+\alpha_1)\ ] + A_2 F[\frac{\pi}{2};\ \mu x(1+\alpha_2)\ ]}{2\pi R} \qquad (2)$$

D = dose rate in mr/h

S_o = source strength in MeV/s (point source)

S_L = source strength in MeV/s · cm (line source)

μ = total gamma ray attenuating coefficient in cm^{-1}

x = shield thickness in cm

$B(\mu x)$ = dose buildup factor

A_1, A_2, α_1, α_2 = Taylor dose buildup coefficients

k = conversion factor from gamma flux to dose rate [3]

R = distance between dose point and source

In these nomograms $R = x$

The values of μ are those given by Grodstein [4], reproduced for instance in ANL 5800 [5]. The values for magnetite concrete are the ones calculated by M. Roos [6] based on μ values given by E. Storm et al. [7].

For points sources the buildup factors used are those given by Goldstein and Wilkins [8]. For concretes the factors for Al have been used. It should be pointed out, however, that there exists later compilations of factors for concrete, for instance, those by Walker and Grotenhuis [9] and by A. Hönig [10]. In the case of ordinary concrete, the results for Al-buildup are slightly inaccurate but at least for the higher gamma energies conservative. In magnetite concrete the Al-buildup gives a very good agreement with that obtained using factors by Walker and Grotenhuis. For the line sources coefficients are taken from the original work by Taylor [11], even these based on data by Goldstein and Wilkins [8]. The Taylor coefficients have also been calculated by Buscaglione and Manzini [12], whose work gives a fit to Goldstein-Wilkins values which is even better than that of the values by Taylor [11].

The error in the buildup calculated by various Taylor coefficients is usually rather small, even in the worst case less than 20 per cent. For line sources and magnetite concrete shields Taylor coefficients for Al have also been used. They give a good agreement with results produced using the values of Walker and Grotenhuis [9].

3. Determination of gamma sources

In order to facilitate the determination of the gamma sources from thermal and epithermal activation and from fission products data from the data library to the program GLAD have been collected here.

The gamma source (S) is given in MeV/g, s per n/cm^2, s in Table 1. If the amount of natural element to be activated is known e.g. in g (m_0) or in g/cm (m_L) and if the activation time = T (hrs), the decay time = t (hrs) and the activating flux (Φ_{th} or Φ_{epi}) are known, then the gamma source is

$$S_0 = S \cdot m_0 \cdot \Phi_{th\ (resp.\ epi)} \cdot (1 - e^{-\lambda T})\, e^{-\lambda t} \qquad (3)$$

$$S_L = S \cdot m_L \cdot \Phi_{th\ (resp.\ epi)} \cdot (1 - e^{-\lambda T})\, e^{-\lambda t} \qquad (4)$$

Here S_0 is a point isotropic source and S_L is a line source. λ is the decay constant in h^{-1} given in Table 1. Φ_{epi} is defined as usual

$$\Phi(E) = \Phi_{epi}/E \qquad (5)$$

If Φ_{th} is given as the total Maxwellian flux (as it is usually done), the cross sections given should be multiplied by a factor of $\sqrt{\pi}/2 = 0.886$. This is due to the fact that the cross sections used in the calculation are the 2200 m/s cross sections. As the uncertainties in most cases are rather large, this correction is normally not necessary and leaving it out gives only a slight overestimate.

For convenience, if methods other than these nomograms are used to determine the shield thickness, the conversion factor from MeV/$/cm^2$, s to mr/h is also given in column 6.

In order to facilitate updating of these data, the basic data used for Table 1 are given in Table 2. These data are in many cases not very well known (only one figure is in many cases significant for the source), because the number of gamma quanta per disintegration is rather uncertain and the cross sections are not so well known either.

In most cases it is unnecessary to calculate the dose from every gamma energy (γ-line) and the user soon gets a feeling about which ones of the lines are significant in a problem of a certain type.

For gamma sources from fission products, the source in MeV/ /sec-W is given in Table 3. S_0 and S_L are given when the operation effect is given in W (P_0) resp. W/cm (P_L), by

$$S_0 = S \cdot P_0 \tag{6}$$

$$S_L = S \cdot P_L \tag{7}$$

The gamma energies, half-lives and the number of quanta per disintegration are taken mainly from Dzhelepov and Peker [13]. Abundances and cross sections are taken from Hughes-Schwartz [14]. The resonance integrals are taken from ANL-5800 [5]. The values in Table 3 are taken from Scoles [15].

4. Determination of the escape probability for a volume source

The escape probability as a function of the dimensions of the source is given in Fig. 1. The values given by Case et al. [16] are used. Due to buildup $\mu\alpha$ will give a too low value and it is recommended to use μe [17]. μa and μe are given for instance in ANL-5800 [5].

5. The use of the nomograms

The procedure for the nomograms appears in Fig. 5. If the distance R between source and dose point is greater than the shield thickness x (Fig. 2) a correction for the geometrical attenuation must be made. In this case a first value x_1 is read, assuming $R = x_1$. Then a new value of x_2 is read with the source strength reduced by the factor $(\frac{x_1}{R})^2$ in the case of a point source and by $(\frac{x_1}{R})$ in the case of line source. This procedure should be repeated once more. If the change in x between the last two values is small enough, the last value of x is the required result. If not, the iteration should be repeated until the difference between the last two values is small enough to be neglected.

5.1 Example 1

We have a gamma source of 10^{11} MeV/s with the gamma energy 1.5 MeV. The geometerical dimension is so small that it can be considered a point source. The escape probability for the source is 0.5 and it is situated 40 cm from the inner surface of the shield. Design an iron shield for a dose rate of 1 mr/h.

To begin with the source strength is reduced by the escape probability giving $5 \cdot 10^{10}$ MeV/s and a shield thickness of 31 cm (Fig. 5, dotted line). The geometrical factor $(\frac{x}{R})^2 = (\frac{31}{40 + 31})^2 = 0.19$. Reducing source strength by this factor we get $9.5 \cdot 10^9$ MeV/s and a shield thickness of 27 cm. Now the new geometrical factor is $(\frac{27}{40 + 27})^2 = 0.16$ and the reduced source strength is $8.0 \cdot 10^9$ MeV/s. The final shield thickness is 26 cm.

5.2 Approximations for handling of finite line sources

As the nomograms are valid for infinite line sources a lower dose rate than specified is obtained for a source of limited length ($\theta < \frac{\pi}{2}$, Fig. 2). Table 4 gives the deviation obtained by replacing a finite line source ($\theta = 10^o - 60^o$) by an infinite line source ($\theta = \frac{\pi}{2}$). The deviation may evidently be neglected.

If the line source is short the spatial variation of the flux will closely approximate that of a point source. Thus for small θ the line source may be replaced by a point source at the center of the line having a source strength $S'_o = S_L \cdot h$ (Fig. 2). The errors involved in this approximation are indicated in Table 5 [2].

As we see in the tables it can be recommended that in normal cases ($\mu x \geq 5$) a line source with $\theta < 20^o$ be replaced by a point source and a line source with $\theta \geq 20^o$ by an infinite line, but to be sure the user should always consult the tables to get the best approximation.

In Figs. 3-12 the nomograms are given for point and line sources for the materials mentioned, Pb in Figs. 3-4, Fe in Figs. 5-6, magnetite concrete in Figs. 7-8, ordinary concrete in Figs. 9-10 and water in Figs. 11-12.

5.3 _ Example 2

In order to demonstrate the computation of the source we give a second example.

Given a rod with 2 cm diameter and a length of 100 cm. The composition is 20 % Cr, 55 % Fe, 0.02 % Co and 25 % Ni. (Weight per cent). The problem is to design an iron shield for a dose rate of 50 mr/h at the surface after an activation with a thermal flux of 10^{13} n/cm^2, s for two weeks (= 336 h).

The computation is made in Table 6.

Formula (4) is used and Table 1. The epithermal flux is considered low enough (say 1/30 of the thermal) that only the thermal activation has to be taken into consideration.

The density of the steel is 7.9 g/cm^3 and thus the amount of steel per cm is 25 g. $P_{esc.}$ is taken from Fig. 1. Ref. 5 gives $\mu e \sim$ ~ 0.035 cm^2/g for E $\sim$ 0.3 MeV and μe 0.025 cm^2/g for E $\sim$ 1 - 1.5 MeV. This gives $\mu e \cdot a = 0.28$ for 0.3 MeV and $\mu e \cdot a = 0.20$ for 1 - 1.5 MeV. Thus we get $P_{esc.} \sim 0.75$ for 0.3 MeV and $P_{esc.} \sim 0.8$ for 1 - 1.5 MeV.

From Fig. 13 it is seen that the dose rate at the surface will be less than 50 mr/h for a shield thickness of 23 cm.

As the angle θ (see Fig. 2) is more than 60^o it is concluded from Table 4 that approximating with an infinite line source is quite satisfactory.

References

1. PIHLAJAVAARA, S E, PIHLMAN, E,
Gamma Attenuation Nomogram for Concrete. Helsinki 1961. (The State Institute for Technical Research Publ. Ser. 3, No. 52).

2. ROCKWELL, T, III, ed.,
Reactor Shielding Design Manual. Princeton, N.J. McGraw. 1956.

3. GOLDSTEIN, H,
Fundamental Aspects of Reactor Shielding. Reading, Mass. Addison-Wesley, 1959.

4. GRODSTEIN, G W,
X-ray Attenuation Coefficients from 10 keV to 100 MeV. 1957. (NBS-C-583) and
GINNÉES, R T,
X-ray Attenuation Coefficients from 10 keV to 100 MeV. 1959. (NBS-C-583-Suppl.).

5. Reactor Physics Constants. 1963. (ANL-5800. 2 ed.)

6. ROOS, M,
Kärnfysikaliska egenskaper hos R3/Adams tunga betong. 1959. (Internal AE-report RSA-17/R3-135). (In Swedish).

7. STORM, E, GILBERT, E , ISRAEL, H,
Gamma-ray Absorption Coefficients for Elements 1 through to 100 Derived from the Theoretical Values of the NBS. 1958. (LA-2237).

8. GOLDSTEIN, H, WILKINS, J E,
Calculations of the Penetration of Gamma Rays. Final report 1954. (NYO-3075).

9. WALKER, R L, GROTENHUIS, M,
A Summary of Shielding Constants for Concrete. 1961. (ANL-6443).

10. HÖNIG, A,
Dosiszuwachsfaktoren bei Beton. Kerntechnik Jahrg 9(1964) 393-399.

11. TAYLOR , J J,
Application of Gamma Ray Build-up Data to Shield Design. 1954. (WAPB-RM-217).

12. BUSCAGLIONE, S, MANZINI, R,
Buil-up Factors: Coefficients of the J.J. Taylor Equation. (Transl. fr the Italian) 1964.(ORNL-TR-80).

13. DZHELEPOV, B S and PEKER, L K,
Decay Schemes of Radioactive Nuclei. Oxf. Pergamon Press, 1961.

14. HUGHES, D J, SCHWARTZ, R B,
Neutron Cross Sections. 2 Ed. 1958. (BNL-325). Suppl. 1. 1960.

15. SCOLES, J F,
Calculated Gamma Ray Spectra from U^{235} Fission Products. 1958. (NARF-58-37T).

16. CASE, K M et al.,
Introduction to the Theory of Neutron Diffusion, Vol. 1 Los Alamos, AEC. 1953.

17. SIDEBOTHAM, E W,
Escape probabilities and fluxes outside selfabsorbing cylindrical sources. Nuclear Power 6 (1961)68-70.

Table 1. γ-sources from activation.

Active isotope	E_γ [MeV]	Saturated γ-source [MeV/g, s per n/cm², s]		λ [h⁻¹]	Conversion factor k [mr/h per MeV/cm², s]
		From thermal activation of natural element (2200 m/s)	From epithermal activation of natural element (≈> 0.4 eV)		
Na^{24}	2.75	3.99, -2	2.2, -2	4.61, -2	1.50, -3
	1.37	1.79, -2	1.0, -2		1.80, -3
Mg^{27}	1.02	2.2, -5	?	4.38	1.91, -3
	0.834	4.1, -5	?		1.98, -3
Al^{28}	1.78	8.35, -3	6.4, -3	1.81, 1	1.70, -3
Si^{31}	1.26	6.0, -8	?	0.265	1.84, -3
Ti^{51}	0.928	3.4, -6	?	7.14	1.95, -3
	0.605	7.5, -7	?		2.06, -3
	0.323	2.7, -5	?		2.02, -3
V^{52}	1.44	7.6, -2	3.7, -2	1.10, 1	1.79, -3
Cr^{51}	0.323	2.6, -4	?	1.04, -3	2.02, -3
Mn^{56}	3.40	1.20, -3	1.4, -3	0.269	1.40, -3
	2.98	1.68, -3	1.9, -3		1.45, -3
	2.66	2.77, -3	3.1, -3		1.50, -3
	2.55	4.80, -3	5.4, -3		1.53, -3
	2.13	5.12, -2	5.8, -2		1.60, -3
	1.81	7.85, -2	8.9, -2		1.69, -3
	0.845	1.36, -1	1.5, -1		1.98, -3
Fe^{59}	1.29	1.82, -5	1.0, -5	6.40, -4	1.84, -3
	1.10	1.95, -5	1.1, -5		1.90, -3
Co^{60}	1.33	4.93, -1	1.0	1.51, -5	1.82, -3
	1.17	4.34, -1	0.9		1.88, -3
Ni^{65}	1.73	1.71, -6	?	2.70, -1	1.70, -3
	1.63	1.75, -6	?		1.73, -3
	1.49	6.76, -5	?		1.78, -3
	1.12	3.25, -5	?		1.89, -3
Cu^{64}	1.34	2.0, -4	2.2, -4	5.41, -2	1.81, -3
Cu^{66}	1.04	4.9, -4	6.0, -4	8.09	1.91, -3
	0.83	9.9, -6	1.2, -5		1.99, -3
Zr^{95}	0.75	6.4, -5	?	4.44, -4	2.00, -3

Zr^{97}	1.84	2.9, -7	?		4.08, -2	1.68, -3
	1.35	3.3, -7	?			1.80, -3
	1.15	3.3, -7	?			1.88, -3
	1.00	2.4, -7	?			1.90, -3
	0.745	6.93, -6	?			2.05, -3
	0.665	6.18, -6	?			2.10, -3
Mo^{99}	0.78	8.9, -5	1.9, -3		1.05, -2	2.00, -3
	0.38	7.4, -6	1.6, -4			2.08, -3
Mo^{101}	2.08	4.0, -5	7.4, -4		3.29	1.62, -3
	1.02	3.1, -5	5.7, -4			1.90, -3
	0.59	1.4, -5	2.6, -4			2.10, -3
Ag^{108}	0.63	9.0, -4	1.5, -3		1.82, 1	2.05, -3
	0.43	1.7, -4	2.8, -4			2.10, -3
Ag^{110m}	1.50	5.7, -3	?	x)	1.07, -4	1.78, -3
	0.94	8.1, -3	?			1.90, -3
	0.76	9.5, -3	?			2.00, -3
Ag^{110}	0.66	1.2, -1	?	x)	1.03, 2	2.08, -3
Cd^{107}	0.85	5.9, -7	?		1.03, -1	1.98, -3
Cd^{115m}	1.30	2.7, -6	?		6.72, -4	1.81, -3
	0.94	4.0, -6	?			1.90, -3
Cd^{115}	0.52	2.4, -4	?		1.30, -2	2.10, -3
Cd^{117m}	1.55	8.3, -5	?		2.38, -1	1.75, -3
	1.27	2.2, -4	?			1.82, -3
	0.84	3.0, -4	?			1.98, -3
	0.43	1.5, -4	?			2.08, -3
In^{114m}	1.3	1.7, -5	?		5.87, -4	1.80, -3
	0.722	3.3, -4	?			2.03, -3
	0.556	2.5, -4	?			2.10, -3
In^{114}	1.30	5.9, -7	?		3.47, 1	1.82, -3
In^{116m}	2.12	4.14, -1	?	xx)	7.69, -1	1.60, -3
	1.51	1.73, -1	?			1.76, -3
	1.30	1.24	?			1.82, -3
	1.10	7.21, -1	?			1.90, -3
	0.82	1.40, -1	?			2.00, -3

Sn^{125m}	1.39	1.5, -6	?	4.29	1.80, -3
	1.07	1.9, -7	?		1.90, -3
	0.640	1.1, -7	?		2.05, -3
	0.326	1.9, -5	?		2.00, -3
Sn^{125}	1.96	8.3, -7	?	2.98, -3	1.65, -3
	1.41	1.4, -7	?		1.80, -3
	1.07	1.9, -6	?		1.90, -3
	0.90	1.3, -6	?		1.95, -3
Sb^{122}	1.26	2.5, -4	6.0, -3	1.04, -2	1.85, -3
	1.14	2.1, -4	5.0, -3		1.90, -3
	0.686	6.3, -4	1.5, -2		2.05, -3
	0.564	1.0, -2	2.4, -1		2.10, -3
Sb^{124}	2.3	2.7, -3	1.5, -1	4.79, -4	1.58, -3
	1.6	5.7, -4	3.1, -2		1.75, -3
	0.97	4.5, -4	2.5, -2		1.90, -3
	0.61	1.6, -3	8.8, -2		2.10, -3
Hf^{181}	0.62	2.2, -5	4.8, -5	6.31, -4	2.10, -3
	0.48	6.0, -3	1.3, -2		2.10, -3
W^{187}	0.89	5.1, -4	5.4, -3	2.9, -2	1.95, -3
	0.78	7.6, -4	8.0, -3		2.00, -3
	0.69	7.7, -3	8.2, -2		2.05, -3
	0.55	1.4, -3	1.5, -2		2.10, -3
	0.48	2.3, -3	2.4, -2		2.10, -3

x) Notice the high resonance integral for activation of Ag^{109}

xx) " " " " " " " " In^{115}

Table 2. For Table 1 used data.

Active isotope	E_γ [MeV]	Quanta per disintegration	Abundance of parent isotope	σ_{act} [b] (2200 m/s)	Σ_{act} [cm^2/g] (g nat. elem) (2200 m/s)	Resonance integral [b]	ρ g/cm^3
Na^{24}	2.75	1.036	1.00	0.536	1.40, -2	0.30±0.05	0.971
	1.37	0.934					
Mg^{27}	1.02	0.299	0.113	0.027	7.1, -5	Mg abs 0.9 ?	1.74
	0.834	0.695					
Al^{28}	1.78	1.0	1.00	0.21	4.69, -3	0.16±0.02	2.70
Si^{30}	1.26	7.0, -4	0.031	0.110	6.85, -5	Si abs 0.5	2.35
Ti^{51}	0.928	4.13, -2	0.053	0.14	9.0, -5	Ti abs ~4	4.5
	0.605	1.38, -2					
	0.323	9.45, -1					
V^{52}	1.44	1.0	0.998	4.5	5.3, -2	~ 2.2	5.96
Cr^{51}	0.323	0.1	0.043	15.9	8.26, -3	Cr abs 2.6 ± 1.1	6.92
Mn^{56}	3.40	2.42, -3	1.00	13.3	1.46, -1	15 ± 1	7.42
	2.98	3.85, -3					
	2.66	7.16, -3					
	2.55	1.29, -2					
	2.13	1.65, -1					
	1.81	2.79, -1					
	0.845	1.10					
Fe^{59}	1.29	0.427	0.0031	1.01	3.3, -5	0.58±0.16	7.86
	1.10	0.538					
Co^{60}	1.33	1	1.00	36.3	3.71, -1	75 ± 5	8.71
	1.17	1					
Ni^{65}	1.73	5.75, -3	0.012	1.52	1.72, -4	Ni abs 3-4	8.75
	1.63	6.25, -3					
	1.49	2.64, -1					
	1.12	1.69, -1					
Cu^{64}	1.34	5.0, -3	0.691	4.51	2.98, -2	5 ± 0.5	8.94
Cu^{66}	1.04	9.1, -2	0.309	1.8	5.2, -3	2.2±0.2	
	0.83	2.3, -3					
Zr^{95}	0.75	1.0	0.174	0.076	8.5, -5	Zr abs 3?	6.44
Zr^{97}	1.84	1.7, -2	0.028	0.053	9.3, -6		
	1.35	2.7, -2					
	1.15	3.1, -2					
	1.00	2.6, -2					

Zr^{97}	0.745	1.00					
	0.665	1.00					
Mo^{99}	0.78	0.15	0.238	0.51	7.4, -4	11 ± 2.5	10.2
	0.38	0.03					
Mo^{101}	2.08	0.16	0.096	0.20	1.2, -4	3.7 ± 0.2	
	1.02	0.25					
	0.59	0.21					
Ag^{108}	0.63	1.1, -2	0.514	45	1.3, -1	74	10.5
	0.43	3.0, -3					
Ag^{110m}	1.50	0.44	0.486	3.2	8.6, -3	(act Ag 109)	
	0.94	1.0					
	0.76	1.38				1200 ± 300	
Ag^{110}	0.66	0.60		113	3.03, -1		
Cd^{107}	0.85	1.0, -2	0.0122	1.0	6.9, -5		8.65
Cd^{115m}	1.30	1.0, -2	0.289	0.14	2.1, -4		
	0.94	2.0, -2					
Cd^{115}	0.52	2.62, -1		1.1	1.7, -3		
Cd^{117m}	1.55	9.0, -2	0.0758	1.5	5.9, -4		
	1.27	3.0, -1					
	0.84	6.0, -1					
	0.43	6.0, -1					
In^{114m}	1.3	1, -3	0.0420	56	1.3, -2	(act In^{113})	7.28
	0.722	3.5, -2				271	
	0.556	3.5, -2					
In^{114}	1.30	1, -3		2.0	4.5, -4		
In^{116m}	2.12	0.251	0.958	155	7.78, -1	(act In^{115})	
	1.51	0.148					
	1.30	1.23				2640 ± 200	
	1.10	0.843					
	0.82	0.222					
Sn^{125m}	1.39	1.9, -2	0.060	0.2	5.8, -5	(act Sn^{124})	7.29
	1.07	3.0, -3				12	
	0.640	3.0, -3					
	0.326	0.997					
Sn^{125}	1.96	3.5, -1		0.004	1.2, -6		
	1.41	8.7, -2					
	1.07	1.5					
	0.90	1.2					

Sb^{122}	1.26	1.0, -2	0.573	6.8	1.9, -2	162 ± 40	6.22
	1.14	1.0, -2					
	0.686	4.8, -2					
	0.564	0.929					
Sb^{124}	2.3	0.22	0.427	2.5	5.2, -3	~ 138 ± 20	
	1.6	0.07					
	0.97	0.09					
	0.61	0.50					
Hf^{181}	0.62	2.90, -3	0.354	10	1.2, -2	21.8	13.3
	0.48	1.04					
W^{187}	0.89	1.87, -2	0.284	34	3.1, -2	360 ± 50	18.9
	0.78	3.13, -2					
	0.69	3.60, -1					
	0.55	8.13, -2					
	0.48	1.56, -1					

Table 3. Fission product γ-sources

Time of operation [hrs]	Energy group [MeV]	Representative energy [MeV]	MeV/sec-W				Conversion factor k [mr/h per MeV/cm², s]
			Time after shut-down [hrs]				
			10^4	10^3	10	0.1	
10^6	0.0-0.5	0.4	1.5,7	5.2,8	4.1,9	8.4,9	2.07,-3
	0.5-0.9	0.7	1.1,9	3.6,9	1.2,10	1.9,10	2.03,-3
	0.9-1.2	1.0	1.2,6	4.5,7	1.3,9	6.8,9	1.93,-3
	1.2-1.6	1.5	2.1,6	5.2,6	1.1,9	1.2,10	1.77,-3
	1.6-2.0	1.8	3.3,5	4.2,8	3.9,9	7.1,9	1.69,-3
	2.0-2.2	2.1	6.1,6	1.5,7	5.8,7	5.5,8	1.62,-3
	2.2-2.6	2.4	2.7,5	7.1,6	2.0,8	3.4,9	1.55,-3
	2.6-3.0	2.7	6.0,4	1.2,5	1.5,6	6.7,8	1.50,-3
	3.0-4.0	3.5	-	3.2,5	6.0,6	1.9,8	1.40,-3
	> 4.0	5.0	-	-	1.7,6	4.8,7	1.26,-3
10^4	0.0-0.5	0.4	9.5,6	5.0,8	4.1,9	8.0,9	2.07,-3
	0.5-0.9	0.7	2.5,8	3.4,9	1.2,10	1.9,10	2.03,-3
	0.9-1.2	1.0	8.0,5	4.5,7	1.3,10	6.7,9	1.93,-3
	1.2-1.6	1.5	1.4,6	2.0,6	1.1,10	1.2,10	1.77,-3
	1.6-2.0	1.8	2.8,5	4.2,8	3.9,9	7.0,9	1.69,-3
	2.0-2.2	2.1	3.9,6	9.5,6	5.5,7	5.4,8	1.62,-3
	2.2-2.6	2.4	1.6,5	7.0,6	2.0,8	3.4,9	1.55,-3
	2.6-3.0	2.7	3.0,4	6.6,4	1.5,6	6.7,8	1.50,-3
	3.0-4.0	3.5	-	3.2,5	6.0,6	1.9,8	1.40,-3
	> 4.0	5.0	-	-	1.7,6	4.8.7	1.26,-3
10^3	0.0-0.5	0.4	1.4,6	3.2,8	3.6,9	7.9,9	2.07,-3
	0.5-0.9	0.7	2.5,7	8.2,8	8.6,9	1.6,10	2.03,-3
	0.9-1.2	1.0	1.2,5	3.1,7	1.3,9	6.7,9	1.93,-3
	1.2-1.6	1.5	2.0,5	5.1,5	1.1,9	1.2,10	1.77,-3
	1.6-2.0	1.8	2.5,4	3.7,8	3.5,9	6.7,9	1.69,-3
	2.0-2.2	2.1	5.8,5	1.5,6	4.3,7	5.3,8	1.62,-3
	2.2-2.6	2.4	2.1,4	5.9,6	1.9,8	3.4,9	1.55,-3
	2.6-3.0	2.7	4.5,3	9.2,3	1.3,6	6.7,8	1.50,-3
	3.0-4.0	3.5	-	2.8,5	5.7,6	1.9,8	1.40,-3
	> 4.0	5.0	-	-	1.7,6	4.8,7	1.26,-3

10^2	0.0-0.5	0.4	1.5,5	5.7,7	1.7,9	6.0,9	2.07,-3
	0.5-0.9	0.7	2.9,6	1.0,8	6.0,9	1.3,10	2.03,-3
	0.9-1.2	1.0	1.4,4	6.4,6	9.1,8	6.4,9	1.93,-3
	1.2-1.6	1.5	2.1,4	6.7,4	1.0,9	1.2,10	1.77,-3
	1.6-2.0	1.8	2.6,3	8.4,7	9.5,8	4.1,9	1.69,-3
	2.0-2.2	2.1	6.1,4	1.5,5	4.1,7	5.3,8	1.62,-3
	2.2-2.6	2.4	2.1,3	1.3,6	1.3,8	3.3,9	1.55,-3
	2.6-3.0	2.7	4.7,2	9.5,2	1.3,6	6.7,8	1.50,-3
	3.0-4.0	3.5	-	6.4,4	3.8,6	1.9,8	1.40,-3
	> 4.0	5.0	-	-	1.7,6	1.8,7	1.26,-3

Table 4. Comparison of doses from infinite line sources and finite line sources.

$$\frac{D_{\theta = \pi/2}}{D_{\theta}}$$

θ	μx = 1	μx = 5	μx = 11	μx = 25
10	5.16	3.05	2.16	1.15
20	2.60	1.60	1.34	1.00
30	1.76	1.22	1.06	1.00
40	1.38	1.06	1.00	1.00
60	1.07	1.00	1.00	1.00

Table 5. Comparison of doses from point sources and line sources.

$$D_{(\text{point source})} / D_{(\text{line source})}$$

θ	μx = 0	μx = 1	μx = 5	μx = 11	μx = 25
1	1.00	1.00	1.00	1.00	1.00
5	1.00	1.00	1.01	1.02	1.04
10	1.01	1.02	1.04	1.07	1.14
20	1.04	1.07	1.15	1.32	1.55
30	1.10	1.16	1.38	1.70	2.37

Table 6. Calculations for example 2 on steel activation.

Element	Weight per cent	γ-energy [MeV]	Saturated γ-source [MeV/g steel, s] Thermal activation	λ T (T=336 h)	$1-e^{-\lambda T}$	γ-source t=0 [MeV/g steel, s]	P_{esc}·γ-source t = 0 [MeV/cm, s]	Dose rate outside the shield [mr/h] 20 cm Fe	25 cm Fe	30 cm Fe
Cr	20	0.323	5.2,8	3.50,-1	0.29	1.5,8	2.8,9	< 1	<0.1	<0.01
Fe	55	1.29	1.0,8	2.15,-1	0.19	1.9,7	3.8,8	8	1	0.1
		1.10	1.1,8			2.1,7	4.2,8	5	0.5	0.05
Co	0.02	1.33	9.9,8	5.08,-3	5.1,-3	5.0,6	1.0,8	4	0.2	0.04
		1.17	8.7,8			4.4,6	8.8,7	1	0.1	0.01
Ni	25	1.73	4.3,6	9.08,1	1	4.6,6	9.2,7	8	0.5	0.1
		1.63	4.4,6			4,4,6	8.8,7	4	0.4	0.08
		1.49	1.7,8			1.7,8	3.4,9	~ 68	~15	2
		1.12	8.1,7			8.1,7	1.6,9	20	2	0.2
							Total	~ 119	~ 20	~2.6

Fig 1. Escape probability versus mean free path in a volume source. a is the radius of the sphere and cylinder and half the thickness of the slab.

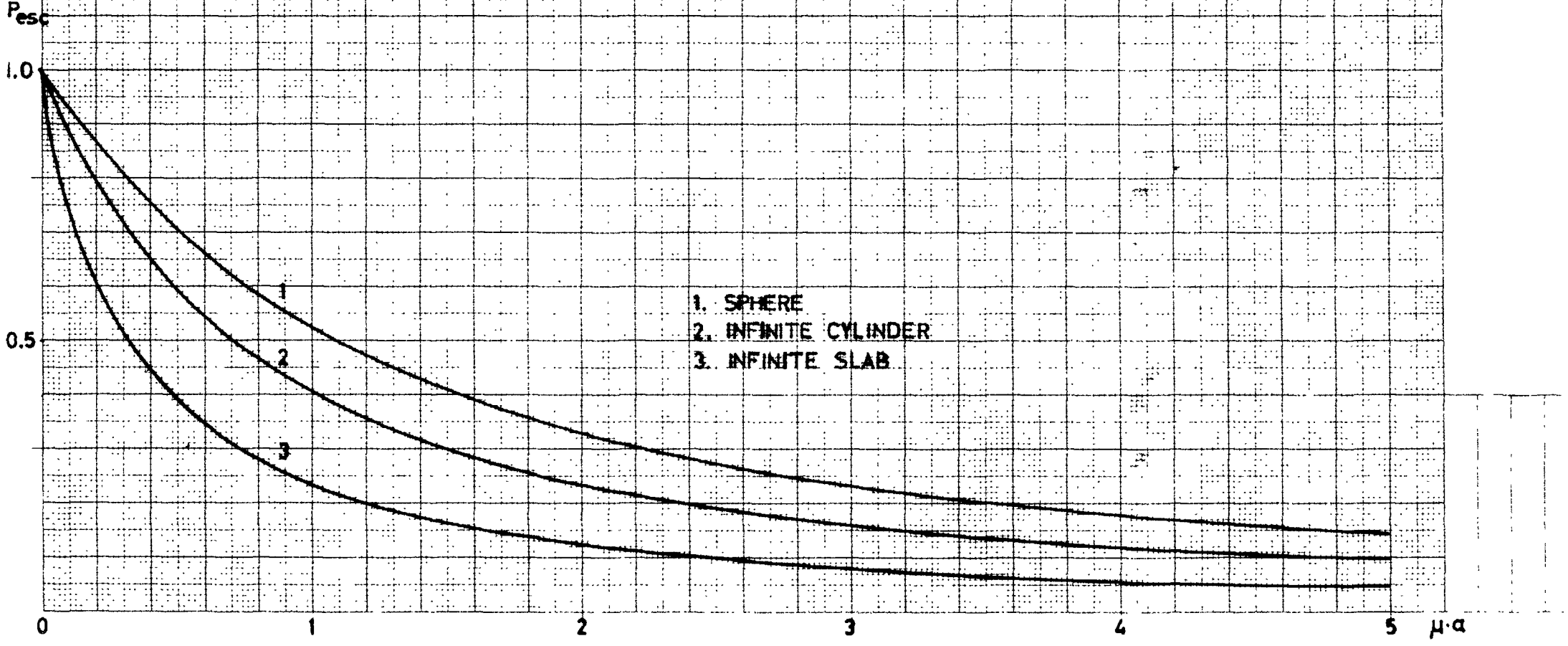

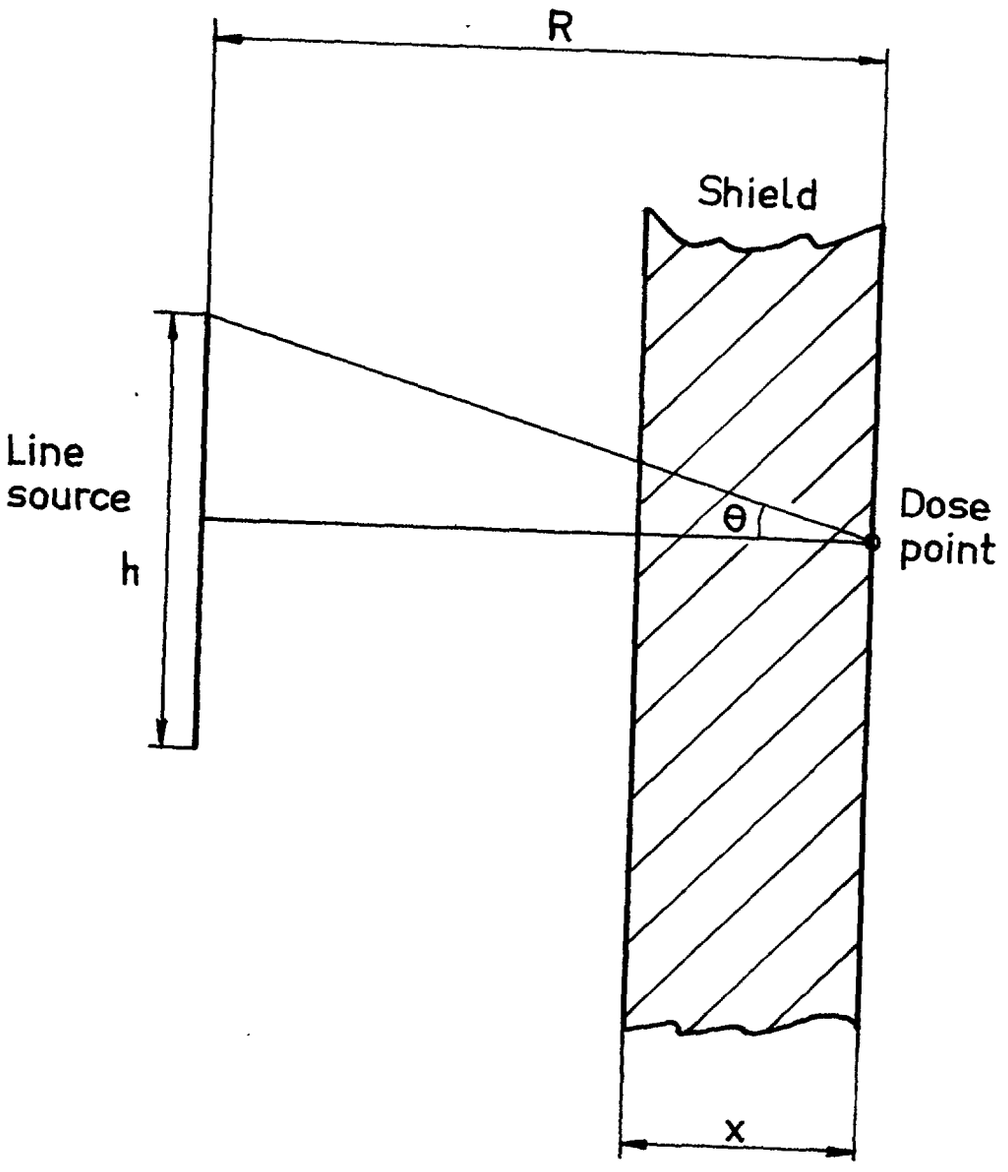

Fig. 2 Shielded line source geometry.

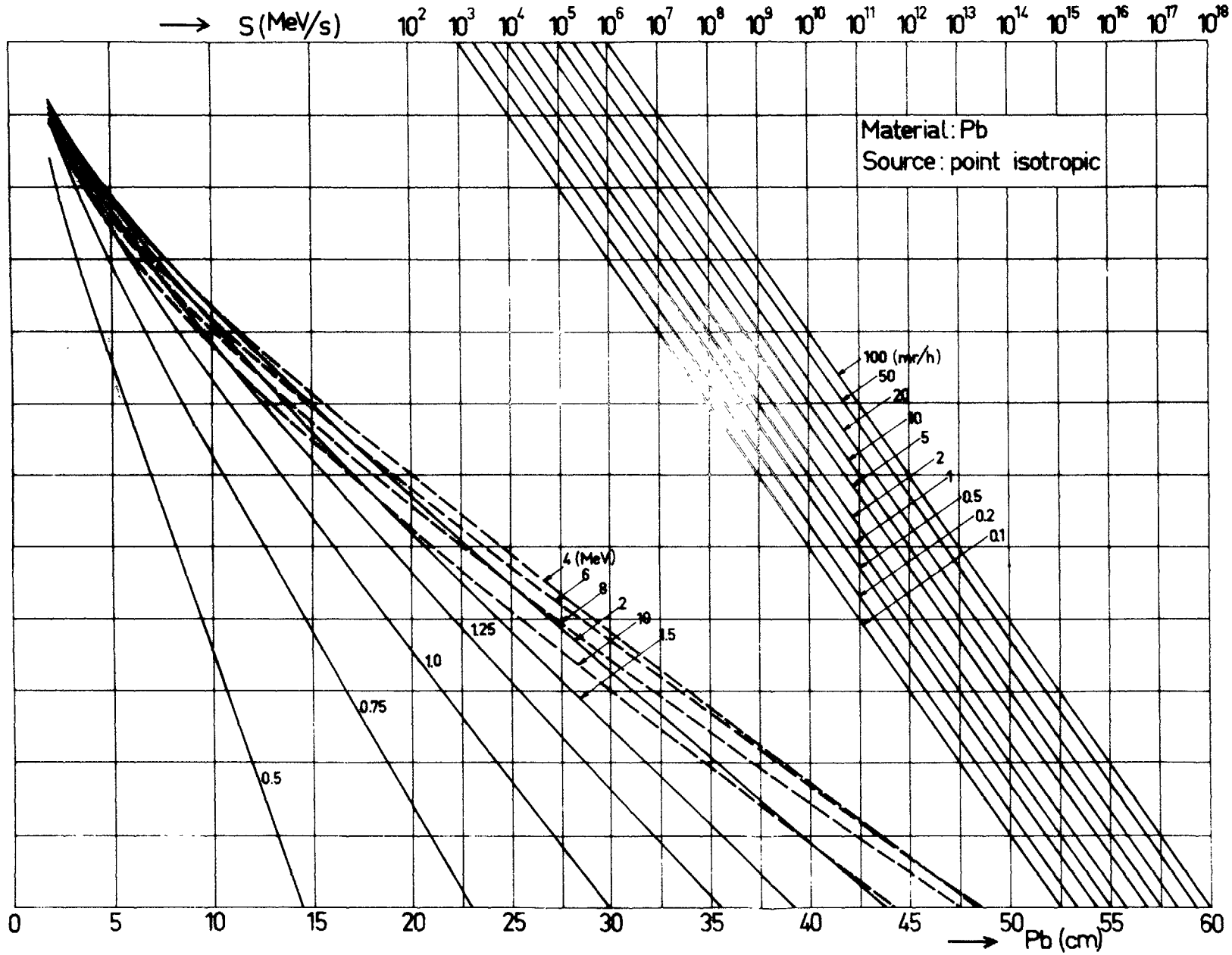

Fig. 3 · Isotropic point source - lead shield

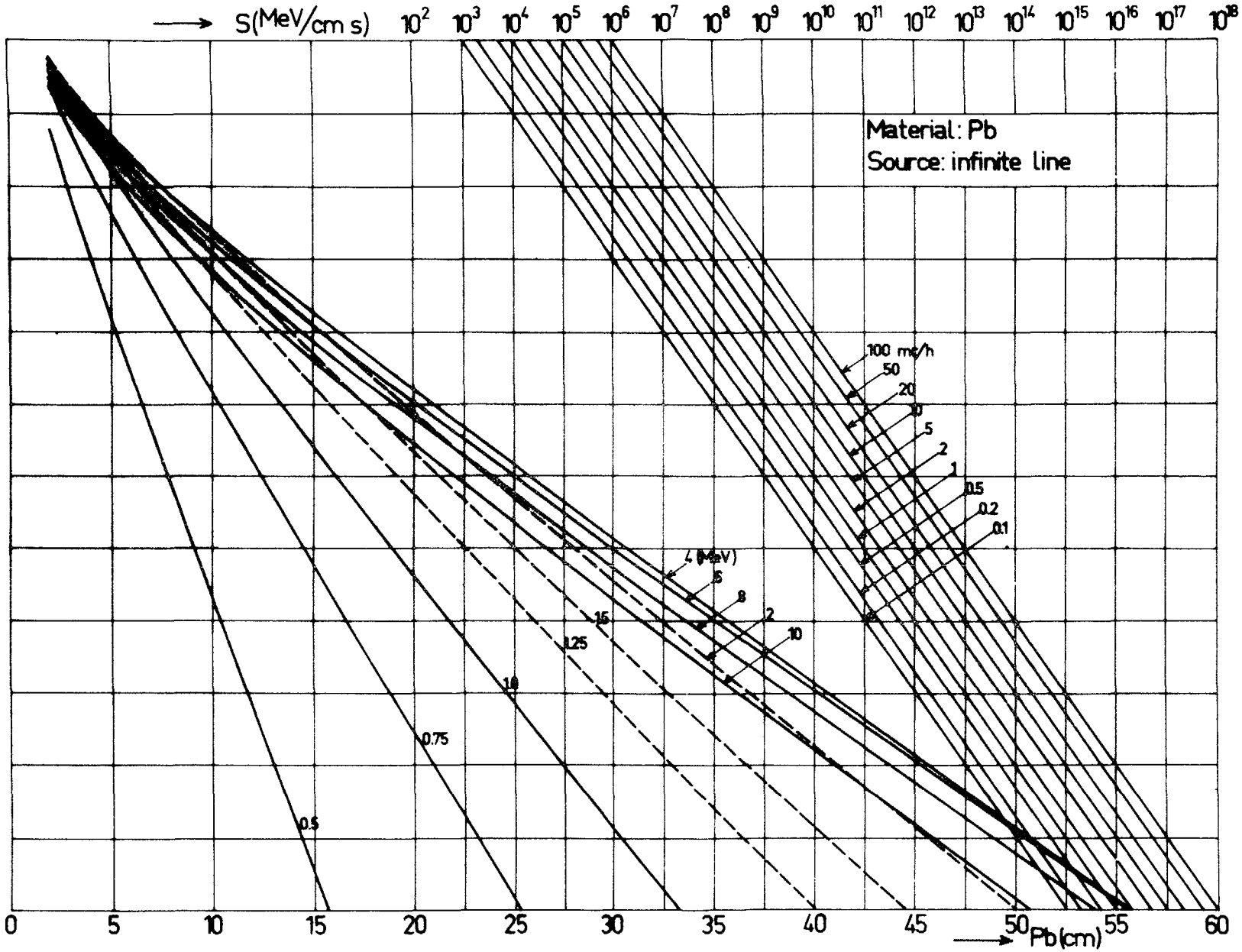

Fig. 4 Infinite line source - lead shield

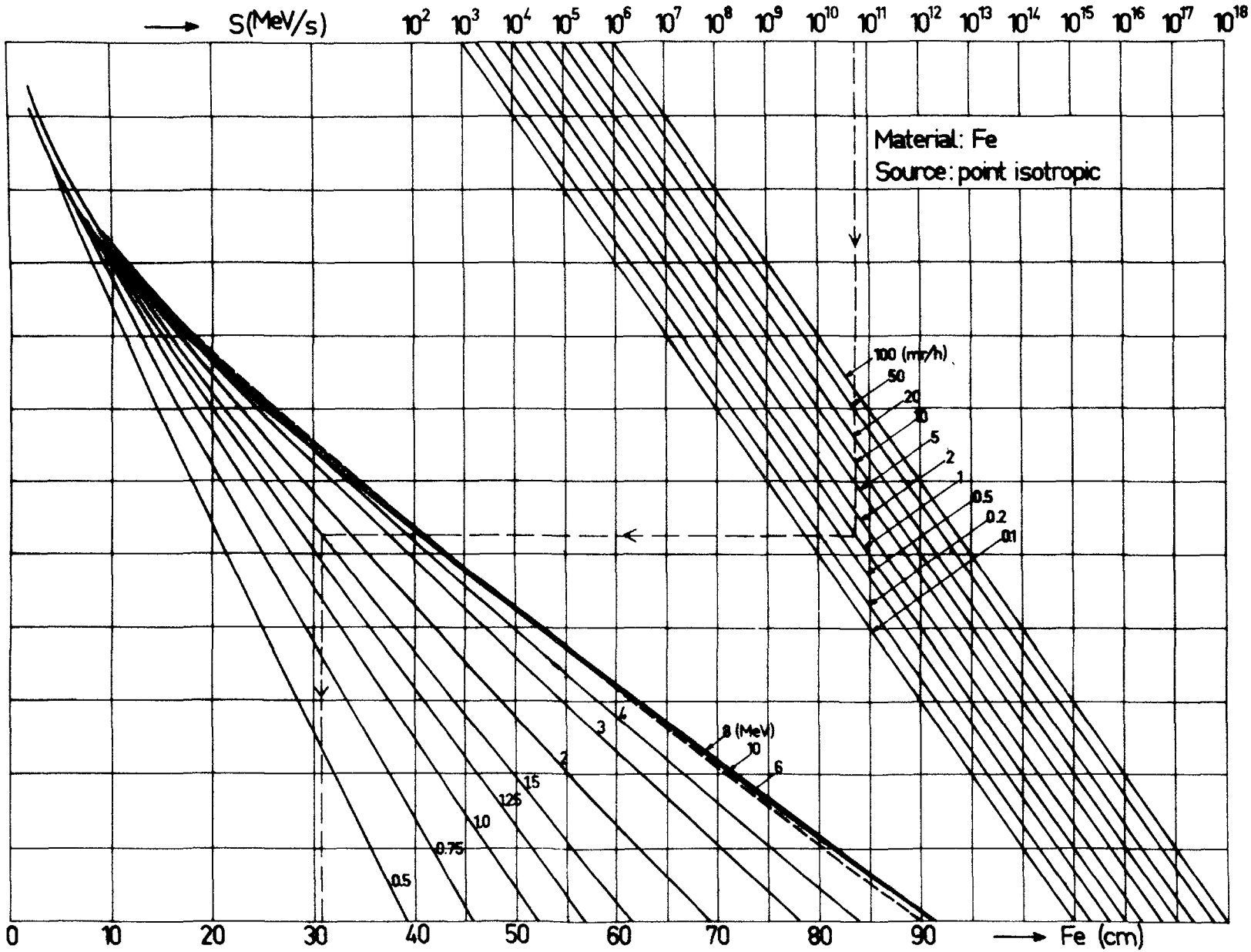

Fig. 5 Isotropic point source - iron shield

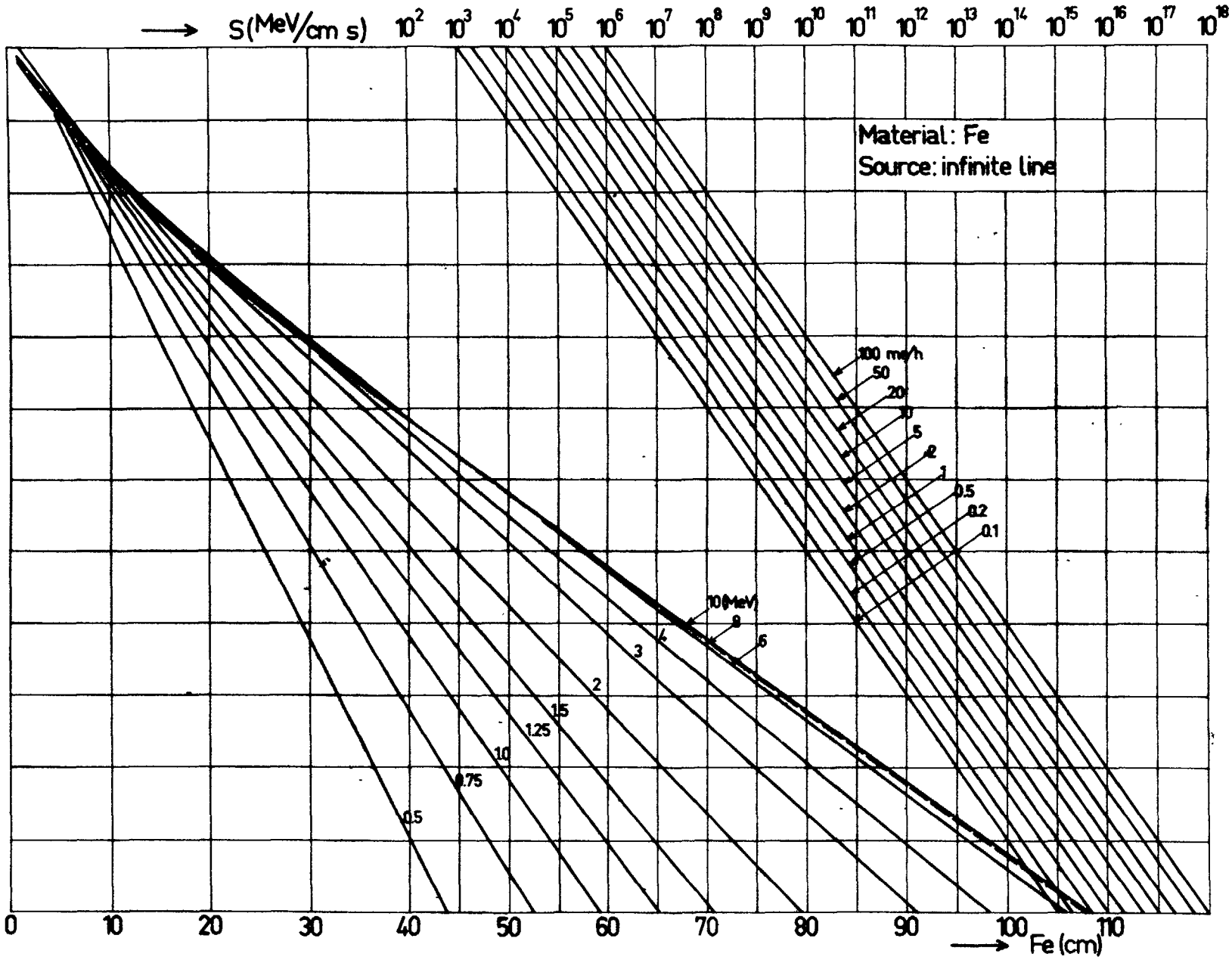

Fig. 6 Infinite line source - iron shield

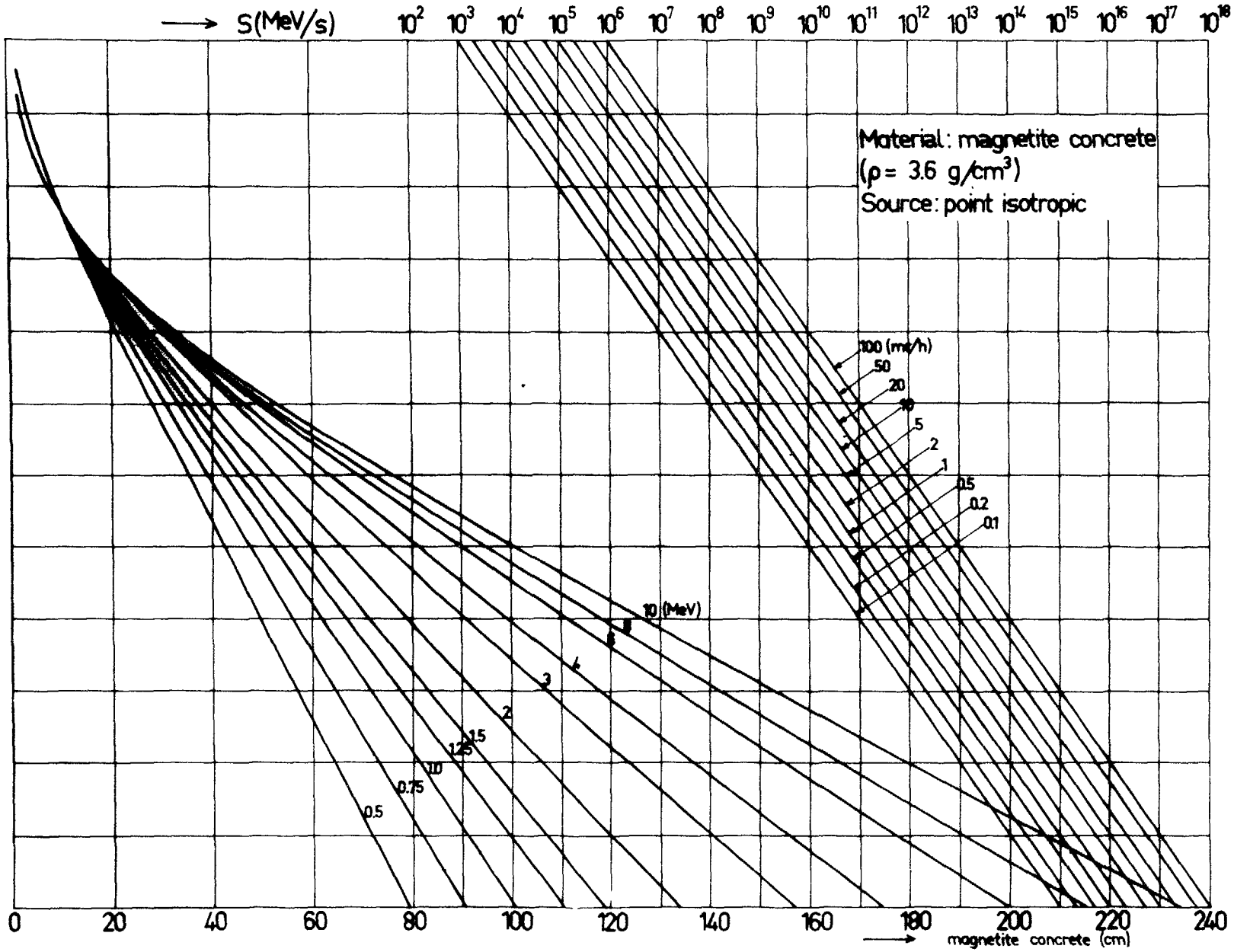

Fig. 7 Isotropic point source - magnetite concrete shield

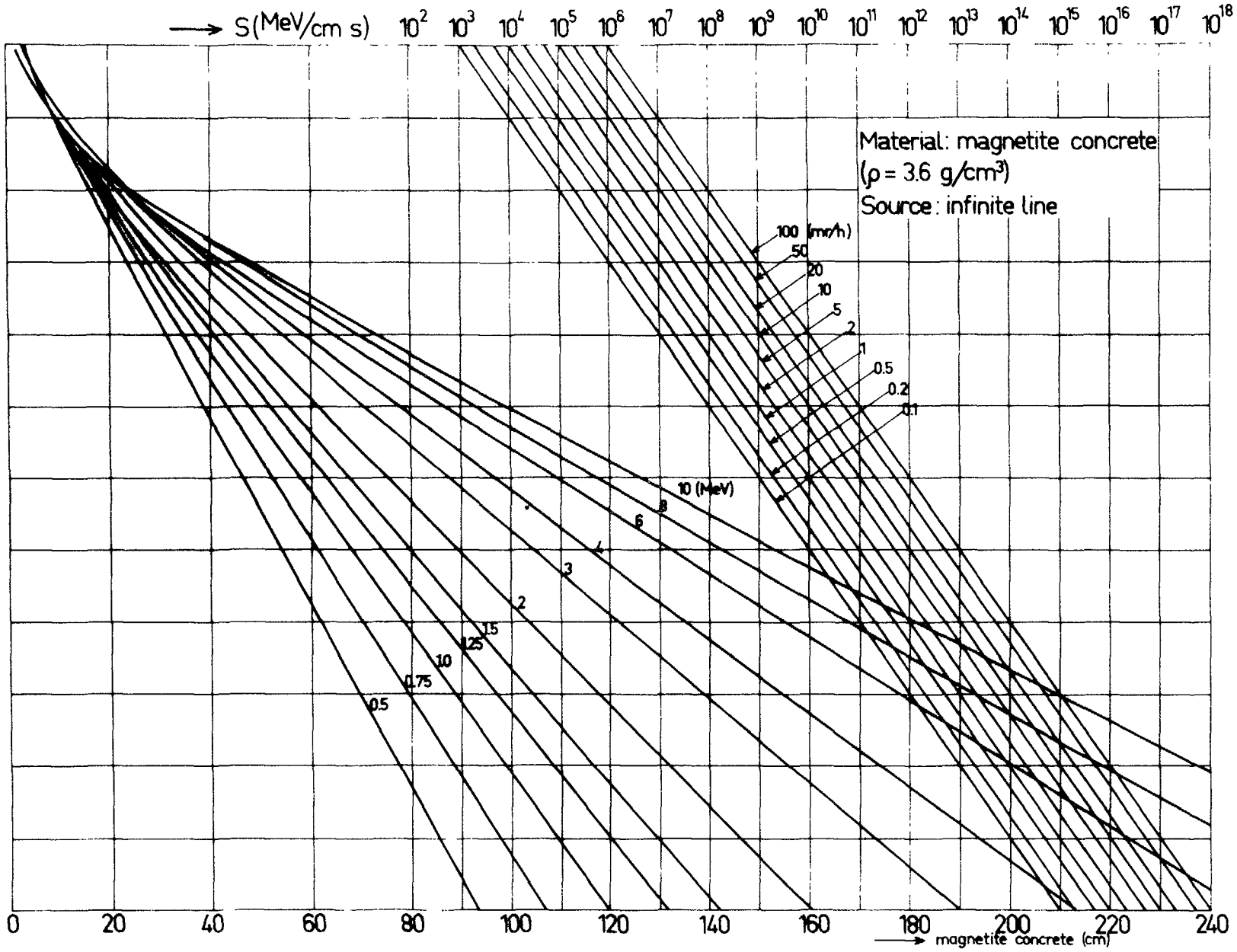

Fig. 8 Infinite line source - magnetite concrete shield

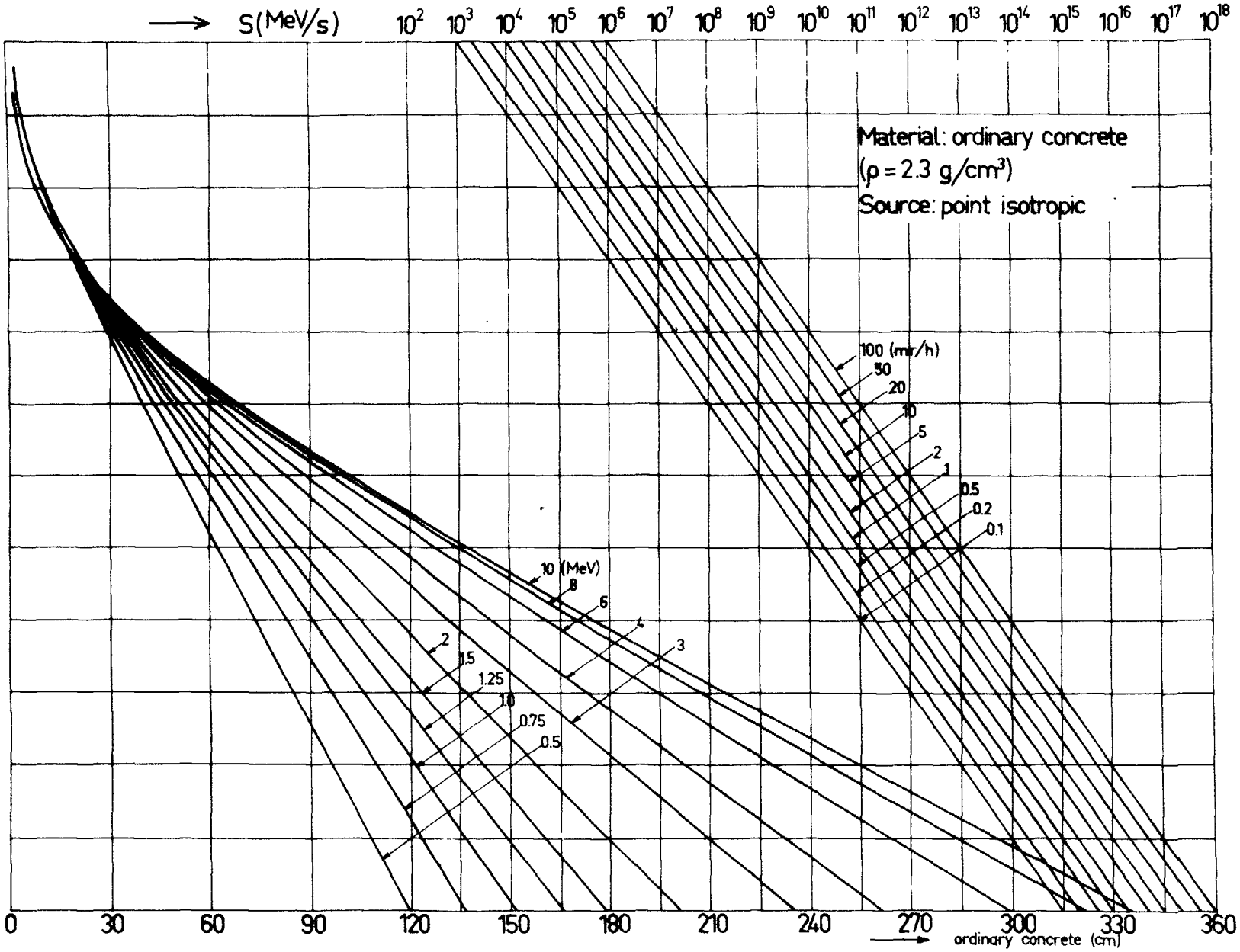

Fig. 9 Isotropic point source - ordinary concrete shield

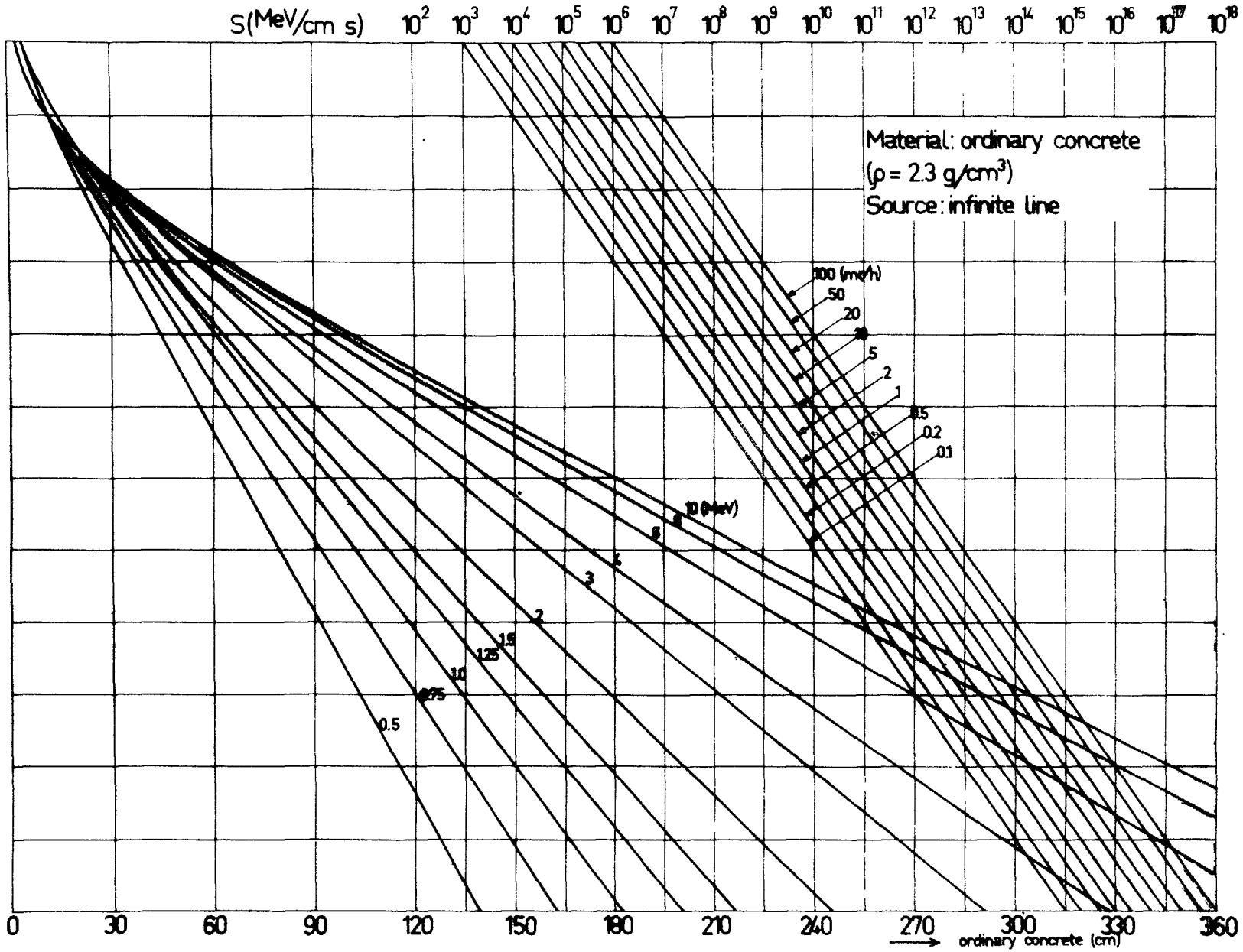

Fig. 10 Infinite line source - ordinary concrete shield

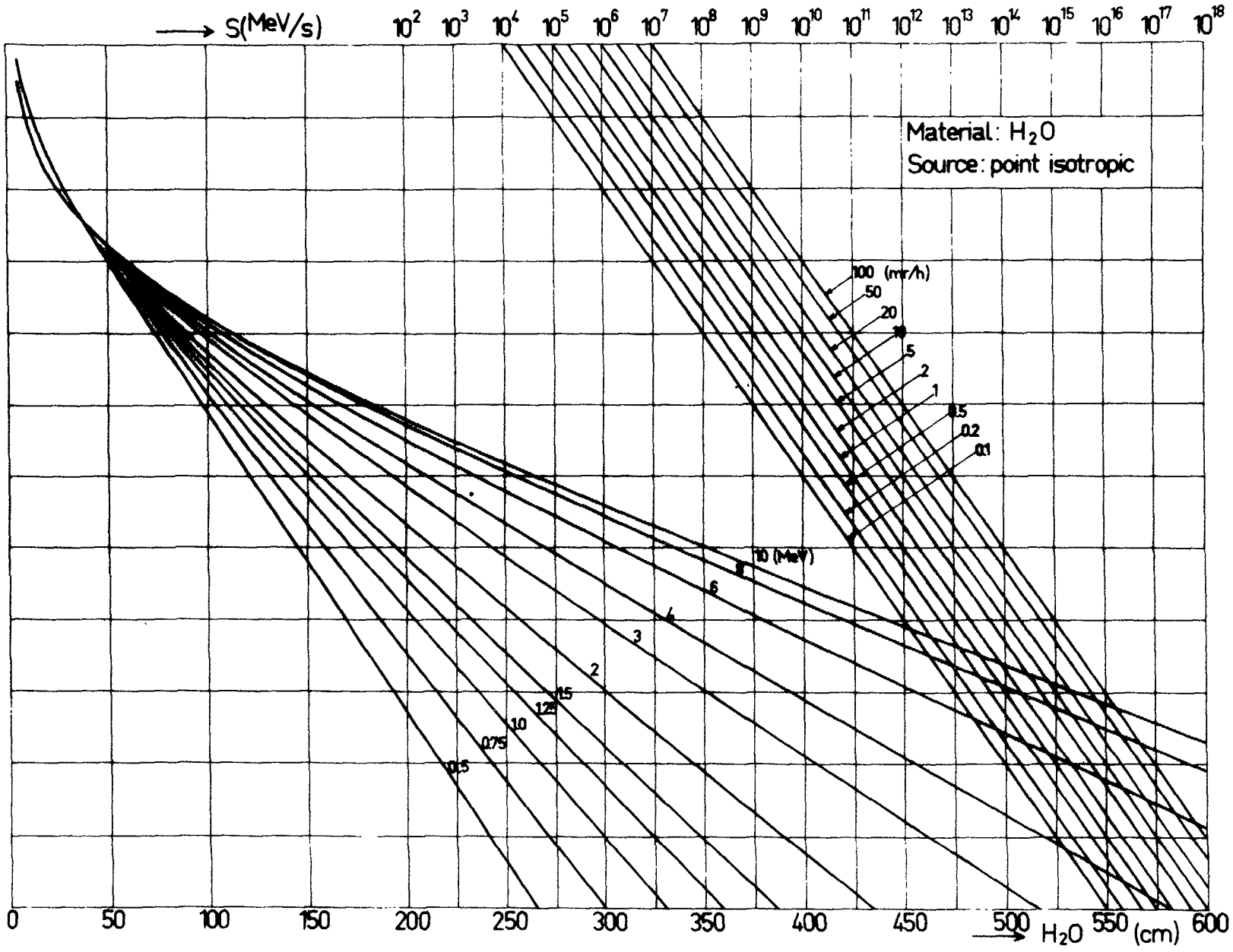

Fig. 11 Isotropic point source - water shield

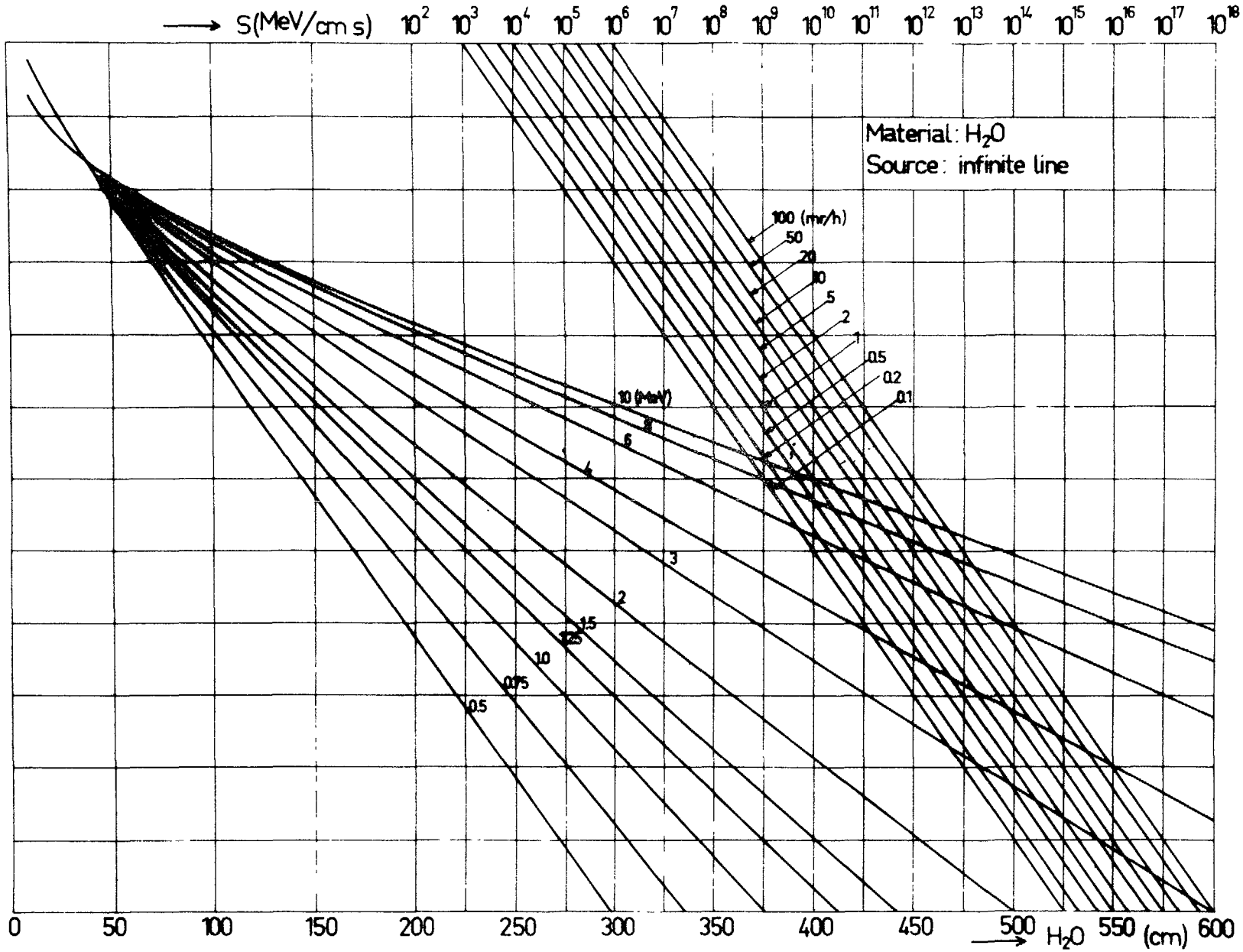

Fig. 12 Infinite line source - water shield

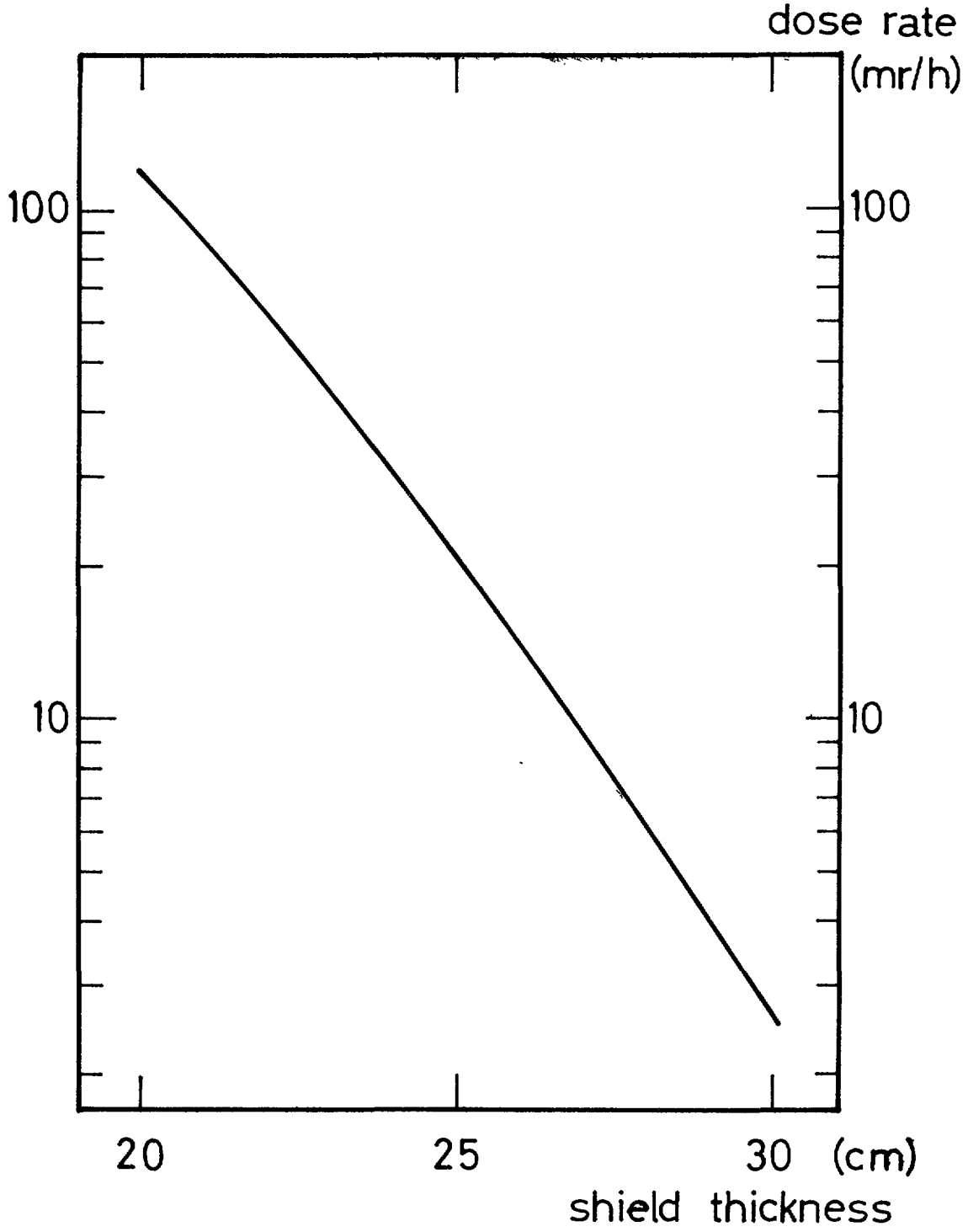

Fig. 13 Dose rate on the shield surface as a function of shield thickness in example 2.

LIST OF PUBLISHED AE-REPORTS

1–170. (See the back cover earlier reports.)

171. Measurements on background and fall-out radioactivity in samples from the Baltic bay of Tvären, 1957–1963. By P. O. Agnedal. 1965. 48 p. Sw. cr. 8:–.

172. Recoil reactions in neutron-activation analysis. By D. Brune. 1965. 24 p. Sw. cr. 8:–.

173. A parametric study of a constant-Mach-number MHD generator with nuclear ionization. By J. Braun. 1965. 23 p. Sw. cr. 8:–.

174. Improvements in applied gamma-ray spectrometry with germanium semiconductor detector. By D. Brune, J. Dubois and S. Hellström. 1965. 17 p. Sw. cr. 8:–.

175. Analysis of linear MHD power generators. By E. A. Witalis. 1965. 37 p. Sw. cr. 8:–.

176. Effect of buoyancy on forced convection heat transfer in vertical channels – a literature survey. By A. Bhattacharyya. 1965. 27 p. Sw. cr. 8:–.

177. Burnout data for flow of boiling water in vertical round ducts, annuli and rod clusters. By K. M. Becker, G. Hernborg, M. Bode and O. Erikson. 1965. 109 p. Sw. cr. 8:–.

178. An analytical and experimental study of burnout conditions in vertical round ducts. By K. M. Becker. 1965. 161 p. Sw. cr. 8:–.

179. Hindered El transitions in Eu^{155} and Tb^{161}. By S. G. Malmskog. 1965. 19 p. Sw. cr. 8:–.

180. Photomultiplier tubes for low level Cerenkov detectors. By O. Strindehag. 1965. 25 p. Sw. cr. 8:–.

181. Studies of the fission integrals of U235 and Pu239 with cadmium and boron filters. By E. Hellstrand. 1965. 32 p. Sw. cr. 8:–.

182. The handling of liquid waste at the research station of Studsvik, Sweden. By S. Lindhe and P. Linder. 1965. 18 p. Sw. cr. 8:–.

183. Mechanical and instrumental experiences from the erection, commissioning and operation of a small pilot plant for development work on aqueous reprocessing of nuclear fuels. By K. Jönsson. 1965. 21 p. Sw cr. 8:–.

184. Energy dependent removal cross-sections in fast neutron shielding theory. By H. Grönroos. 1965. 75 p. Sw. cr. 8:–.

185. A new method for predicting the penetration and slowing-down of neutrons in reactor shields. By L. Hjärne and M. Leimdörfer. 1965. 21 p. Sw. cr. 8:–.

186. An electron microscope study of the thermal neutron induced loss in high temperature tensile ductility of Nb stabilized austenitic steels. By R. B. Roy. 1965. 15 p. Sw. cr. 8:–.

187. The non-destructive determination of burn-up means of the Pr-144 2.18 MeV gamma activity. By R. S. Forsyth and W. H. Blackadder. 1965. 22 p. Sw. cr. 8:–.

188. Trace elements in human myocardial infarction determined by neutron activation analysis. By P. O. Wester. 1965. 34 p. Sw. cr. 8:–.

189. An electromagnet for precession of the polarization of fast-neutrons. By O. Aspelund, J. Björkman and G. Trumpy. 1965. 28 p. Sw. cr. 8:–.

190. On the use of importance sampling in particle transport problems. By B. Eriksson. 1965. 27 p. Sw. cr. 8:–.

191. Trace elements in the conductive tissue of beef heart determined by neutron activation analysis. By P. O. Wester. 1965. 19 p. Sw. cr. 8:–.

192. Radiolysis of aqueous benzene solutions in the presence of inorganic oxides. By H. Christensen. 12 p. 1965. Sw. cr. 8:–.

193. Radiolysis of aqueous benzene solutions at higher temperatures. By H. Christensen. 1965. 14 p. Sw. cr. 8:–.

194. Theoretical work for the fast zero-power reactor FR-0. By H. Häggblom. 1965. 46 p. Sw. cr. 8:–.

195. Experimental studies on assemblies 1 and 2 of the fast reactor FR0. Part 1. By T. L. Andersson, E. Hellstrand, S-O. Londen and L. I. Tirén. 1965. 45 p. Sw. cr. 8:–.

196. Measured and predicted variations in fast neutron spectrum when penetrating laminated Fe-D_2O. By E. Aalto, R. Sandlin and R. Fräki. 1965. 20 p. Sw. cr. 8:–.

197. Measured and predicted variations in fast neutron spectrum in massive shields of water and concrete. By E. Aalto, R. Fräki and R. Sandlin. 1965. 27 p. Sw. cr. 8:–.

198. Measured and predicted neutron fluxes in, and leakage through, a configuration of perforated Fe plates in D_2O. By E. Aalto. 1965. 23 p. Sw. cr. 8:–.

199. Mixed convection heat transfer on the outside of a vertical cylinder. By A. Bhattacharyya. 1965. 42 p. Sw. cr. 8:–.

200. An experimental study of natural circulation in a loop with parallel flow test sections. By R. P. Mathisen and O. Eklind. 1965. 47 p. Sw. cr. 8:–.

201. Heat transfer analogies. By A. Bhattacharyya. 1965. 55 p. Sw. cr. 8:–.

202. A study of the "384" KeV complex gamma emission from plutonium-239. By R. S. Forsyth and N. Ronqvist. 1965. 14 p. Sw. cr. 8:–.

203. A scintillometer assembly for geological survey. By E. Dissing and O. Landström. 1965. 16 p. Sw. cr. 8:–.

204. Neutron-activation analysis of natural water applied to hydrogeology. By O. Landström and C. G. Wenner. 1965. 28 p. Sw. cr. 8:–.

205. Systematics of absolute gamma ray transition probabilities in deformed odd-A nuclei. By S. G. Malmskog. 1965. 60 p. Sw. cr. 8:–.

206. Radiation induced removal of stacking faults in quenched aluminium. By U. Bergenlid. 1965. 11 p. Sw. cr. 8:–.

207. Experimental studies on assemblies 1 and 2 of the fast reactor FR0. Part 2. By E. Hellstrand, T. Andersson, B. Brunfelter, J. Kockum, S-O. Londen and L. I. Tirén. 1965. 50 p. Sw. cr. 8:–.

208. Measurement of the neutron slowing-down time distribution at 1.46 eV and its space dependence in water. By E. Möller. 1965. 29 p. Sw. cr. 8:–.

209. Incompressible steady flow with tensor conductivity leaving a transverse magnetic field. By E. A. Witalis. 1965. 17 p. Sw. cr. 8:–.

210. Methods for the determination of currents and fields in steady two-dimensional MHD flow with tensor conductivity. By E. A. Witalis. 1965. 13 p. Sw. cr. 8:–.

211. Report on the personnel dosimetry at AB Atomenergi during 1964. By K. A. Edvardsson. 1966. 15 p. Sw. cr. 8:–.

212. Central reactivity measurements on assemblies 1 and 3 of the fast reactor FR0. By S-O. Londen. 1966. 58 p. Sw. cr. 8:–.

213. Low temperature irradiation applied to neutron activation analysis of mercury in human whole blood. By D. Brune. 1966. 7 p. Sw. cr. 8:–.

214. Characteristics of linear MHD generators with one or a few loads. By E. A. Witalis. 1966. 16 p. Sw. cr. 8:–.

215. An automated anion-exchange method for the selective sorption of five groups of trace elements in neutron-irradiated biological material. By K. Samsahl. 1966. 14 p. Sw. cr. 8:–.

216. Measurement of the time dependence of neutron slowing-down and thermalization in heavy water. By E. Möller. 1966. 34 p. Sw. cr. 8:–.

217. Electrodeposition of actinide and lanthanide elements. By N-E. Bärring. 1966. 21 p. Sw. cr. 8:–.

218. Measurement of the electrical conductivity of He^3 plasma induced by neutron irradiation. By J. Braun and K. Nygaard. 1966. 37 p. Sw. cr. 8:–.

219. Phytoplankton from Lake Magelungen, Central Sweden 1960–1963. By T. Willén. 1966. 44 p. Sw. cr. 8:–.

220. Measured and predicted neutron flux distributions in a material surrounding av cylindrical duct. By J. Nilsson and R. Sandlin. 1966. 37 p. Sw. cr. 8:–.

221. Swedish work on brittle-fracture problems in nuclear reactor pressure vessels. By M. Grounes. 1966. 34 p. Sw. cr. 8:–.

222. Total cross-sections of U, UO_2 and ThO_2 for thermal and subthermal neutrons. By S. F. Beshai. 1966. 14 p. Sw. cr. 8:–.

223. Neutron scattering in hydrogenous moderators, studied by the time dependent reaction rate method. By L. G. Larsson, E, Möller and S. N. Purohit. 1966. 26 p. Sw. cr. 8:–.

224. Calcium and strontium in Swedish waters and fish, and accumulation of strontium-90. By P-O. Agnedal. 1966. 34 p. Sw. cr. 8:–.

225. The radioactive waste management at Studsvik. By R. Hedlund and A. Lindskog. 1966. 14 p. Sw. cr. 8:–.

226. Theoretical time dependent thermal neutron spectra and reaction rates in H_2O and D_2O. S. N. Purohit. 1966. 62 p. Sw. cr. 8:–.

227. Integral transport theory in one-dimensional geometries. By I. Carlvik. 1966. 65 p. Sw. cr. 8:–.

228. Integral parameters of the generalized frequency spectra of moderators. By S. N. Purohit. 1966. 27 p. Sw. cr. 8:–.

229. Reaction rate distributions and ratios in FR0 assemblies 1, 2 and 3. By T. L. Andersson. 1966. 50 p. Sw. cr. 8:–.

230. Different activation techniques for the study of epithermal spectra, applied to heavy water lattices of varying fuel-to-moderator ratio. By E. K. Sokolowski. 1966. 34 p. Sw. cr. 8:–.

231. Calibration of the failed-fuel-element detection systems in the Ågesta reactor. By O. Strindehag. 1966. 52 p. Sw. cr. 8:–.

232. Progress report 1965. Nuclear chemistry. Ed. by G. Carleson. 1966. 26 p. Sw. cr. 8:–.

233. A Summary Report on Assembly 3 of FR0. By T. L. Andersson, B. Brunfelter, P. F. Cecchi, E. Hellstrand, J. Kockum, S-O. Londen and L. I. Tirén. 1966. 34 p. Sw. cr. 8:–.

234. Recipient capacity of Tvären, a Baltic Bay. By P.-O. Agnedal and S. O. W. Bergström. 21 p. Sw. cr. 8:–.

235. Optimal linear filters for pulse height measurements in the presence of notise. By K. Nygaard. 16 p. Sw. cr. 8:–.

236. DETEC, a subprogram for simulation of the fast-neutron detection process in a hydro-carbonous plastic scintillator. By B. Gustafsson and O. Aspelund. 1966. 26 p. Sw. cr. 8:–.

237. Microanalys of fluorine contamination and its depth distribution in zircaloy by the use of a charged particle nuclear reaction. By E. Möller and N. Starfelt. 1966. 15 p. Sw. cr. 8:–.

238. Void measurements in the regions of sub-cooled and low-quality boiling. P. 1. By S. Z. Rouhani. 1966. 47 p. Sw. cr. 8:–.

239. Void measurements in the regions of sub-cooled and low-quality boiling. P. 2. By S. Z. Rouhani. 1966. 60 p. Sw. cr. 8:–.

240. Possible odd parity in ^{129}Xe. By L. Broman and S. G. Malmskog. 1966. 10 p. Sw. cr. 8:–.

241. Burn-up determination by high resolution gamma spectrometry: spectra from slightly-irradiated uranium and plutonium between 400–830 keV. By R. S. Forsyth and N. Ronqvist. 1966. 22 p. Sw. cr. 8:–.

242. Half life measurements in ^{155}Gd. By S. G. Malmskog. 1966. 10 p. Sw. cr. 8:–.

243. On shear stress distributions for flow in smooth or partially rough annuli. By B. Kjellström and S. Hedberg. 1966. 66 p. Sw. cr. 8:–.

244. Physics experiments at the Ågesta power station. By G. Apelqvist, P.-Å. Bliselius, P. E. Blomberg, E. Jonsson and F. Åkerhielm. 1966. 30 p. Sw. cr. 8:–.

245. Intercrystalline stress corrosion cracking of inconel 600 inspection tubes in the Ågesta reactor. By B. Grönwall, L. Ljungberg, W. Hübner and W. Stuart. 1966. 26 p. Sw. cr. 8:–.

246. Operating experience at the Ågesta nuclear power station. By S. Sandström. 1966. 113 p. Sw. cr. 8:–.

247. Neutron-activation analysis of biological material with high radiation levels. By K. Samsahl. 1966. 15 p. Sw. cr. 8:–.

248. One-group perturbation theory applied to measurements with void. By R. Persson. 1966. 19 p. Sw. cr. 8:–.

249. Optimal linear filters. 2. Pulse time measurements in the presence of noise. By K. Nygaard. 1966. 9 p. Sw. cr. 8:–.

250. The interaction between control rods as estimated by second-order one-group perturbation theory. By R. Persson. 1966. 42 p. Sw. cr. 8:–.

251. Absolute transition probabilities from the 453.1 keV level in 183W. By S. G. Malmskog. 1966. 12 p. Sw. cr. 8:–.

252. Nomogram for determining shield thickness for point and line sources of gamma rays. By C. Jönemalm and K. Malén. 1966. 33 p. Sw. cr. 8:–.

Förteckning över publicerade AES-rapporter

1. Analys medelst gamma-spektrometri. Av D. Brune. 1961. 10 s. Kr 6:–.
2. Beströlningsförändringar och neutronatmosfär i reaktortrycktankar – några synpunkter. Av M. Grounes. 1962. 33 s. Kr 6:–.
3. Studium av sträckgränsen i mjukt stål. Av G. Östberg och R. Attermo. 1963. 17 s. Kr 6:–.
4. Teknisk upphandling inom reaktorområdet. Av Erik Jonson. 1963. 64 s. Kr 8:–.
5. Ågesta Kraftvärmeverk. Sammanställning av tekniska data, beskrivningar m. m. för reaktordelen. Av B. Lilliehöök. 1964. 336 s. Kr 15:–.
6. Atomdagen 1965. Sammanställning av föredrag och diskussioner. Av S. Sandström. 1966. 321 s. Kr 15:–.

Additional copies available at the library of AB Atomenergi, Studsvik, Nyköping, Sweden. Micronegatives of the reports are obtainable throught Filmprodukter, Gamla landsvägen 4, Ektorp, Sweden.

EOS-tryckerierna, Stockholm 1966